Haploinsufficiency of a Spliceosomal GTPase Encoded by *EFTUD2* Causes Mandibulofacial Dysostosis with Microcephaly

Matthew A. Lines,[1] Lijia Huang,[1] Jeremy Schwartzentruber,[2] Stuart L. Douglas,[1] Danielle C. Lynch,[1] Chandree Beaulieu,[1] Maria Leine Guion-Almeida,[3] Roseli Maria Zechi-Ceide,[3] Blanca Gener,[4] Gabriele Gillessen-Kaesbach,[5] Caroline Nava,[6] Geneviève Baujat,[6] Denise Horn,[7] Usha Kini,[8] Almuth Caliebe,[9] Yasemin Alanay,[10,11] Gulen Eda Utine,[10] Dorit Lev,[12] Jürgen Kohlhase,[13] Arthur W. Grix,[14] Dietmar R. Lohmann,[15] Ute Hehr,[16] Detlef Böhm,[13] FORGE Canada Consortium,[17] Jacek Majewski,[18] Dennis E. Bulman,[19] Dagmar Wieczorek,[15,20] and Kym M. Boycott[1,20,*]

Mandibulofacial dysostosis with microcephaly (MFDM) is a rare sporadic syndrome comprising craniofacial malformations, microcephaly, developmental delay, and a recognizable dysmorphic appearance. Major sequelae, including choanal atresia, sensorineural hearing loss, and cleft palate, each occur in a significant proportion of affected individuals. We present detailed clinical findings in 12 unrelated individuals with MFDM; these 12 individuals compose the largest reported cohort to date. To define the etiology of MFDM, we employed whole-exome sequencing of four unrelated affected individuals and identified heterozygous mutations or deletions of *EFTUD2* in all four. Validation studies of eight additional individuals with MFDM demonstrated causative *EFTUD2* mutations in all affected individuals tested. A range of *EFTUD2*-mutation types, including null alleles and frameshifts, is seen in MFDM, consistent with haploinsufficiency; segregation is de novo in all cases assessed to date. U5-116kD, the protein encoded by *EFTUD2,* is a highly conserved spliceosomal GTPase with a central regulatory role in catalytic splicing and post-splicing-complex disassembly. MFDM is the first multiple-malformation syndrome attributed to a defect of the major spliceosome. Our findings significantly extend the range of reported spliceosomal phenotypes in humans and pave the way for further investigation in related conditions such as Treacher Collins syndrome.

Mandibulofacial dysostosis (MFD) is a disturbance in the development of the first and second branchial arches and causes malar and mandibular hypoplasia, a cleft palate, and/or conductive hearing loss. Although several distinct MFD syndromes are recognized, the most well understood is Treacher Collins syndrome (MIM 154500), a common, isolated form caused by mutations of three genes involved in pre-rRNA transcription.[1,2] Of the several other recognized mandibulofacial and acrofacial dysostoses, only the gene associated with Miller syndrome (MIM 263750) has been identified; this gene encodes an enzyme involved in pyrimidine biosynthesis.[3] Etiologies of the remaining MFD syndromes remain unknown.

In 1996, Guion-Almeida et al.[4] described four individuals with a distinct sporadic syndrome (MIM 610536) combining MFD with microcephaly, growth and developmental delay, a cleft palate, and characteristic external ear malformations with preauricular tags. Two subsequent reports[5,6] described a total of five phenotypically similar individuals, and the inheritance pattern was again sporadic with the exception of a single affected mother and son.[6] To further delineate the phenotype of this condition, which we have provisionally termed "MFD with microcephaly" (MFDM), we assembled a cohort of 12 unrelated affected individuals, including five previously reported persons.[4,5] The phenotype of all 12 individuals with MFDM (Table 1; Figure 1) is characterized by microcephaly, midface hypoplasia, micrognathia, and a characteristic external ear appearance. Microcephaly in this condition is both progressive and severe and might be of either pre- or postnatal onset. A significant deceleration of head growth is seen during infancy, and head circumference eventually falls to between 3 and 6 standard deviations (SD) below the mean. All affected individuals

[1]Children's Hospital of Eastern Ontario Research Institute, University of Ottawa, Ottawa, Ontario K1H 8L1, Canada; [2]McGill University and Genome Quebec Innovation Centre, Montréal, Québec H3A 1A4, Canada; [3]Department of Clinical Genetics, Hospital for Rehabilitation of Craniofacial Anomalies, University of São Paulo, Bauru 17012-900, Brazil; [4]Clinical Genetics, Department of Pediatrics, Hospital Universitario Cruces, Baracaldo, Vizcaya 48903, Spain; [5]Universitätsklinikum Schleswig-Holstein, Campus Lübeck, Lübeck 23538, Germany; [6]Département de Genetique, Centre de Référence Maladies Osseuses Constitutionnelles, Hôpital Necker-Enfants Malades, Paris 75015, France; [7]Institute of Medical and Human Genetics, Charité, Berlin 13353, Germany; [8]Department of Clinical Genetics and the Spires Cleft Lip and Palate Centre, Oxford Radcliffe Hospitals National Health Service Trust, Oxford OX3 7LJ, UK; [9]Institute of Human Genetics, University of Kiel, Kiel 24105, Germany; [10]Pediatric Genetics Unit, Department of Pediatrics, Hacettepe University Faculty of Medicine, Ankara 06532, Turkey; [11]Pediatric Genetics Unit, Department of Pediatrics, Acibadem University, Istanbul 34457, Turkey; [12]Institute of Medical Genetics, Wolfson Medical Center, Holon 58100, Israel; [13]Center for Human Genetics Freiburg, Freiburg 79100, Germany; [14]Genetics, Kaiser Permanente, Sacramento, CA 95815, USA; [15]Institut für Humangenetik, Universitaetsklinikum Essen, Essen 45147, Germany; [16]Department of Human Genetics, University of Regensburg, Regensburg 93053, Germany; [17]FORGE Steering Committee Membership is listed in Acknowledgments; [18]Department of Human Genetics, McGill University, Montréal, Québec H3A 1B1, Canada; [19]Ottawa Hospital Research Institute, Ottawa, Ontario K1Y 4E9, Canada
[20]These authors contributed equally to this work
*Correspondence: kboycott@cheo.on.ca
DOI 10.1016/j.ajhg.2011.12.023.

Table 1. Phenotype of Individuals with MFDM

	Individual											
	1	**2**	**3**	**4**	**5**	**6**	**7**	**8**	**9**	**10**	**11**	**12**
Reference	this report	Wieczorek[5], "patient 2"	Wieczorek[5], "patient 3"	Guion-Almeida[4], "patient 2"	this report	this report	Wieczorek[5], "patient 1"	this report	Guion-Almeida[4], "patient 1"	this report	this report	this report
Inheritance	sporadic	sporadic	sporadic	sporadic	sporadic	sporadic	sporadic	sporadic	sporadic	sporadic	sporadic	sporadic
Sex	M	M	F	M	F	M	F	F	M	M	F	M
Consanguinity	-	-	-	-	-	-	-	-	+ (f = 1/16)	-	-	-
Paternal age (years)	35	N/R	N/R	28	N/R	26	N/R	31	25	N/R	N/R	N/R
Pregnancy complications	N/R	N/R	increased NT and microcephaly	N/R	IUGR	N/R	PROM	-	-	-	poly-hydramnios	increased NT
Gestation (weeks)	37	42	39	full term (number of weeks not available)	40	39	33	41+3	full term (number of weeks not available)	40	41+4	42
Birth weight (g)	2,150 (−2 SD)	3,180 (−1.5 SD)	2,850 (−1.25 SD)	3,100	2,610 (−2 SD)	2,400 (−2.5 SD)	1,500 (−1.5 SD)	3,870 (+0.5 SD)	3,500	3,000 (−1 SD)	3,330 (−1 SD)	3,161 (−1.5 SD)
Birth head circumference (cm)	30.5 (−1.75 SD)	33 (−2 SD)	30 (−3 SD)	N/R	31 (−2.75 SD)	N/R	27 (−2 SD)	32.5 (−2 SD)	N/R	33 (−1 SD)	31 (−3.5 SD)	N/R
Age at last assessment	3 years	7 years, 8 months	6 years, 5 months	9 years, 5 months	2 years, 7 months	1 year, 2 months	7 years, 2 months	2 years	13 years, 4 months	2 years, 5 months	1 year	7 years, 2 months
Head circumference (cm)	(−3.5 SD)	47 (−3.5 SD)	43.8 (−5 SD)	48 (−3.5 SD)	43.5 (−4 SD)	43 (−3 SD)	42.5 (−6 SD)	42 (−5 SD)	50 (−3 SD)	44.5 (−4 SD)	39.8 (−5 SD)	46.4 (4 years, 9 months) (−3 SD)
Weight (kg)	normal	24 (+0 SD)	22.5 (+0 SD)	24 (−2 SD)	13.4 (+0 SD)	8 (−3.5 SD)	24 (+0 SD)	10.3 (−2 SD)	38 (−1.5 SD)	12.7 (−0.75 SD)	6.72 (−4 SD)	22.6 (7 years, 2 months) (+0 SD)
Height (cm)	normal	122 (−1 SD)	117.4 (+0 SD)	131 (−1 SD)	87 (−1.75)	71 (−3 SD)	118 (−1 SD)	84 (−0.25 SD)	151 (−1.25 SD)	89 (−0.75 SD)	69 (−2 SD)	116.6 (7 years, 2 months) (−1.5 SD)
Malar hypoplasia	+	+	+	+	+	+	+	+	+	+	-	+
Micrognathia	+	+	+	+	+	+	+	+	+	+	+	+
Obliquity of palpebrae	upslanting	upslanting	level	one downslanting	upslanting	downslanting	upslanting	downslanting	+	level	level	level
Lower-eyelid cleft	-	+	-	-	-	-	-	-	-	+	bilateral	-
Microtia	+	+	+	+	+	+	+	+	+	+	+	N/R
Preauricular tags	+	unilateral	bilateral	+	unilateral	unilateral	unilateral	-	+	unilateral	-	unilateral
Auditory canal atresia or stenosis	N/R	bilateral	unilateral	-	unilateral	N/R	bilateral	+	-	bilateral	unilateral	-
Hearing loss	conductive	conductive	conductive	N/A	conductive	sensorineural	conductive	conductive	-	conductive	conductive	conductive

Table 1. ***Continued***

	Individual											
	1	**2**	**3**	**4**	**5**	**6**	**7**	**8**	**9**	**10**	**11**	**12**
Midline cleft palate (including submucous)	-	+	-	+	+	bifid uvula	-	-	+	+	+	-
Choanal atresia	+	bilateral	unilateral	-	N/R	N/R	bilateral	bilateral	-	-	-	bilateral
Need for neonatal resuscitation	+	-	-	-	-	+	+	-	-	-	-	-
Tracheostomy	+	-	-	-	-	-	-	-	-	-	-	-
Global developmental delay	+	mild to moderate	mild	moderate to severe	moderate to severe	+	moderate	moderate	severe	mild to moderate	mild to moderate	moderate
Age at walking (months)	28	16	24	17	24–36	N/R	24	24	60	19	NM	19
Age at first words (months)	NM	24	20	24	NM	N/R	30	NM	NM	NM	NM	N/R
Brain MRI	normal	delayed myelination at 15 months of age	normal	N/R	N/R	N/R	N/R	N/R	N/R	abnormal white matter on FLAIR	N/R	N/R
Seizures	N/R	+	-	+	-	N/R	+	-	+	+	-	-
Gastrostomy	+	-	+	-	-	-	-	-	-	N/R	-	-
Metopic ridge	+	+	-	+	+	+	-	-	+	N/R	-	+
Congenital heart defect	-	ASD	-	-	VSD	ASD	mild PPS	-	ASD	ASD	ASD	-
Proximally placed thumb	+	-	+	N/R	N/R	+	-	-	N/R	N/R	-	+
Duplicated thumb	-	-	-	-	-	-	-	-	+	N/R	-	-
Other anomalies	cryptorchidism and small scrotum	hypoplastic toenails and delayed bone age	myopia, middle ear and vestibular hypoplasia	-	-	cryptorchidism and small scrotum	-	-	-	N/R	-	-
Karyotype	46,XY	N/R	46,XX	46,XY	46,XX	N/R	46,XX	46,XX	46,XY	46,XY	46,XX	46,XY
Microarray (hg19)	see Table 2	normal	N/R	N/R	see Table 2	N/R	N/R	normal	N/R	normal	N/R	normal
EFTUD2 mutation (see Table 2)	deletion of last nine exons	p.Arg262Trp	p.Gln924*	p.Ser586fs*19	complex rearrangement causing deletion	p.Arg262fs*1	p.Ser391fs*57	p.Gln719*	p.Tyr831*	intron 16 5′ splice site	p.Leu637Arg	p.Cys476Arg

Abbreviations are as follows: N/R, not reported; NT, nuchal translucency; IUGR, intrauterine growth restriction; PROM, premature rupture of membranes; N/A, not assessed; NM, milestone not yet met; FLAIR, fluid attenuated inversion recovery; ASD, atrial septal defect; VSD, ventricular septal defect; and PPS, peripheral pulmonic stenosis.

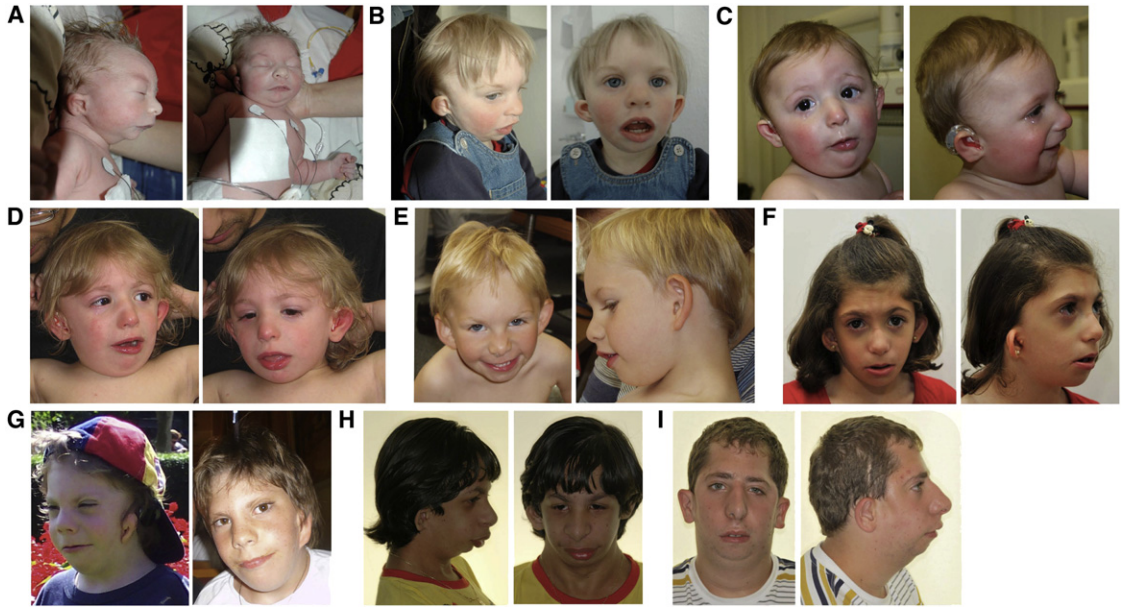

Figure 1. Characteristic Craniofacial Dysmorphism in MFDM
The detailed clinical description of these individuals is reported in Table 1. Typical findings include a sloping forehead, malar hypoplasia, micrognathia, a wide mouth, and a characteristic external ear appearance (preauricular tags, microtia, a small superior helix, and a prominent lobe with a square posterior margin). Microtia is variable in severity; some patients have a cupped ear configuration.
(A) Individual 11: birth
(B) Individual 11: 19 months
(C) Individual 8: 8 months
(D) Individual 8: 24 months
(E) Individual 12: 7 years
(F) Individual 3: 6 years, 5 months
(G) Individual 2: 3.5 years (left) and 10.5 years (right)
(H) Individual 9: 13 years, 5 months
(I) Individual 4: 16 years, 8 months

identified to date have shown significant global developmental delay, and expressive language is particularly affected (only half of our cohort has attained any speech whatsoever; first words are generally spoken between 20 and 30 months). Of the four individuals who have had brain imaging, magnetic resonance imaging (MRI) was normal in two, whereas nondiagnostic abnormalities (delayed myelination or nonspecific white-matter changes) were seen in the other two individuals. Additional commonly seen major malformations included choanal and aural atresia, cleft palate, and congenital heart defects (typically atrial septal defects), and each was present in more than half of the affected individuals. Hearing loss, generally conductive, was reported in 10 of the 12 individuals. Minor anomalies that were inconsistently observed included cryptorchidism and proximally placed thumbs. Despite the scarcity of prior clinical reports, the multiplicity of findings in our cohort is such that we consider MFDM to be a distinct, clinically recognizable syndrome.

To determine the genetic basis of MFDM, we performed exome capture and high-throughput sequencing of four unrelated affected individuals. We obtained approval of the study design from the institutional research ethics board (Children's Hospital of Eastern Ontario), and informed consent was obtained from responsible persons (parents) on behalf of all study participants. We performed target enrichment by using the Agilent SureSelect 50 Mb All Exon Kit, and sequencing (Illumina Hiseq) generated >12 Gbp of 100 bp paired-end reads per sample. Variant calling and annotation were performed as follows (see Web Resources): Reads were preprocessed (trimmed), and sequences with a matching (opposite) read were aligned to hg19 with Burrows-Wheeler Aligner.[7] Duplicate reads were marked with Picard and were excluded. Single-nucleotide variants and short in/dels were called with SAMtools pileup and varFilter[8] and were quality-filtered so that at least 20% of the reads supported the variant call. We annotated the variants by using Annovar[9] and custom scripts to select coding and splice-site variants and to exclude common ($\geq$1% minor allele frequency) polymorphisms represented in dbSNP131, the 1000 Genomes pilot release, or in 120 local exomes performed at our center. We performed genome-wide copy-number analysis in parallel for each of the four affected individuals by microarray (Illumina Human Omni2.5).

We next tabulated the rare variants seen in our cohort and compared them between the probands to prioritize genes of interest. Because the mode of inheritance of MFDM was not known a priori, our data were considered under both an autosomal-dominant (one variant per

Table 2. Rare-Variant Analysis in Individuals with MFDM[a]

Any X of Four Individuals	1	2	3	4
Genes containing missense, nonsense, in/del, or splice-site variants	2,523	196	18	2
Allele frequency of ≤1% in dbSNP131, 1000 Genomes, and 120 local exomes	1,474	161	8[b]	1 (*MUC4*)[c]

[a] With a dominant model of disease.
[b] Including *EFTUD2*.
[c] Private *MUC4* variants are a frequent finding at our center; therefore, this gene was deliberately excluded from further analysis.

gene per proband) and an autosomal-recessive (two variants per gene per proband) model. Apart from *MUC4* (a frequent "false positive" in whole-exome studies at our center), no genes satisfied a recessive model in all four probands after filtering; therefore, an identifiable recessive locus for MFDM was deemed unlikely. Next, applying a dominant model, we noted that eight genes contained variants in three out of four MFDM exomes (Table 2). Of these eight genes, one (*EFTUD2*) was noted to have a region of reduced read depth in the remaining (fourth) proband (Figure 2); microarray confirmed a corresponding deletion of the last nine exons of *EFTUD2* in this individual. To verify *EFTUD2* as the gene associated with MFDM, we analyzed *EFTUD2* in a further eight individuals with MFDM. We identified heterozygous mutations in seven cases, and in the eighth individual, we found a complex de novo chromosomal rearrangement causing heterozygous deletion of *EFTUD2* (Table 3, Figure 2, and Figures S1 and S2). A wide variety of mutation types, including large deletions, frameshifts, and splice-site, nonsense, and missense mutations, were observed, consistent with haploinsufficiency. Mutations were not represented in more than 10,000 exomes contained within the National Heart, Lung, and Blood Institute (NHLBI) Exome Variant Server (see Web Resources), and they were determined to be de novo in all seven cases in which parental samples were obtainable. Taken together, our findings are consistent with de novo haploinsufficiency of *EFTUD2* as the cause of MFDM in all cases assessed to date.

Because 2 of the 12 members in our cohort were found to have a microdeletion identifiable on the array, we next considered the spectrum of normal variation within *EFTUD2*. The Database of Genomic Variants does not contain any copy-number variants overlapping *EFTUD2*. Additionally, neither dbSNP nor the Exome Variant Server contains any truncating single-nucleotide polymorphisms within this gene. DECIPHER does contain one individual (249945) bearing a small deletion overlapping *EFTUD2* and two adjacent genes, but the phenotype of this individual is not specified. *EFTUD2* deletions or truncating mutations are therefore not represented in existing catalogs of normal genomic variation in the general population.

EFTUD2 encodes U5-116kD, a highly conserved spliceosomal GTPase with striking sequence similarity to the ribosomal translation elongation factor EF-2.[10] The domain architecture of U5-116kD is comparable to that of other EF-related proteins, consisting of a GTP-binding domain and additional conserved domains II–V; both U5-116kD and its (better known) *S. cerevisiae* homolog, Snu114p, also have a N-terminal acidic domain of unknown function not present in other members of this family.[10] Although there are currently no reported phenotypes for *EFTUD2* in metazoa, the functions of both U5-116kD and Snu114p have been thoroughly characterized. In the spliceosome, Snu114p occupies a central position within the U4/U6-U5 tri-snRNP particle,[11] where it forms a stable

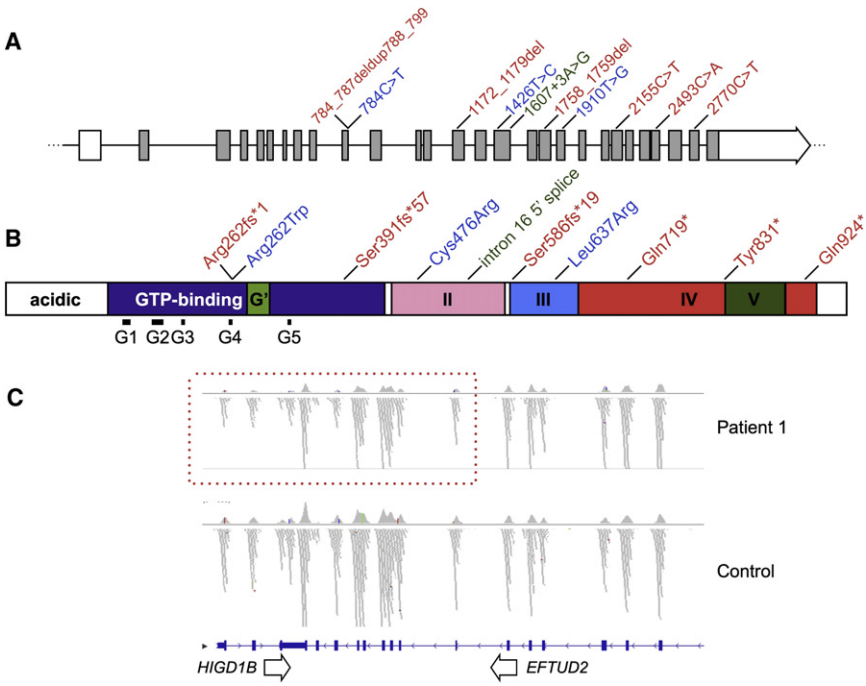

Figure 2. Locations of Disease-Causing Mutations in *EFTUD2*
(A) Intron-exon structure of *EFTUD2* (introns not to scale) with the locations of ten MFDM-causing point mutations (relative to NM_004247.3). Missense mutations are shown in blue, truncating (nonsense and frameshift) mutations are shown in red, and the intron 16 splice-donor mutation is shown in green.
(B) Domain architecture of U5-116kDa (after Fabrizio et al., 1997)[7] indicates the locations of point mutations (the color scheme is the same as that in A).
(C) Exome-sequencing read depth in proband 1 shows a zone of reduced coverage (dashed box) extending from exons 20–29 of *EFTUD2* into the adjoining gene (*HIGD1B*). A corresponding microdeletion was confirmed by microarray (coordinates are listed in Table 3).

Table 3. *EFTUD2* Mutations and Deletions in Individuals with MFDM

Individual	Nucleotide	Peptide	Inheritance	Predicted Effect
1[a]	chr17: 42923422–42935059 × 1		N/A	deletion of last nine exons
2[a]	c.784C>T	p.Arg262Trp	de novo	missense
3[a]	c.2770C>T	p.Gln924*	de novo	nonsense
4[a]	c.1758_1759del	p.Ser586fs*19	N/A	frameshift
5	chr17: 42792021–43147305 × 1 chr17: 41993587–42253276 × 3 chr4: 59109311–59427079 × 1		de novo	deletion affecting 11 genes (including *EFTUD2*); duplication of a further ten genes
6	c.784_787deldup788_799 TGATCCTGGAGC	p.Arg262fs*1	N/A	frameshift
7	c.1172_1179del	p.Ser391fs*57	de novo	frameshift
8	c.2155C>T	p.Gln719*	de novo	nonsense
9	c.2493C>A	p.Tyr831*	de novo	nonsense
10	c.1607+3A>G	p.Tyr537fs*25 (predicted)	N/A	5′ splice site, intron 1[b]
11	c.1910T>G	p.Leu637Arg	de novo	missense
12	c.1426T>C	p.Cys476Arg	N/A	missense

cDNA positions given are relative to NM_004247.3. Chromosome reference positions are relative to hg19. Primer sequences and sequencing chromatograms are provided in Table S1 and Figure S1. Chromosome rearrangements in individuals 1 and 5 are depicted in Figure S2. The following abbreviation is used: N/A, not Assessed.
[a] Discovery (exome) cohort participant.
[b] Predicted in silico to abolish splicing (see Web Resources).

complex with two catalytically essential RNA helicases, Brr2p and Prp8p.[12] Snu114p is essential for Brr2p-mediated dissociation of U4 and U6 RNAs; this dissociation is a key event during catalytic splicing.[13] After splicing, Snu114p is also required for the disassembly and subunit recycling of the postsplicing intron complex; a model has been proposed in which Snu114p acts as a central "GTP switch" regulating both splicing and disassembly.[14] In keeping with this important role in gene expression, Snu114p is an essential yeast protein, alterations of which cause temperature-sensitive growth arrest accompanied by the accumulation of unspliced transcripts.[15,16] Interestingly, all three of the *EFTUD2* missense mutations (resulting in amino acid substitutions p.Arg262Trp, p.Cys478Arg, and p.Leu637Arg) seen in our cohort occur at (or adjacent to) corresponding Snu114p temperature-sensitive alterations (p.Asp271Asn, p.Arg487Glu, and p.Asp653Val, respectively) in yeast.[15,16] A U5-116kD structural model (Figure 3) based on the crystal structure of *S. cerevisiae* EF-2[17] places these three alterations in disparate domains of the protein; Arg262 is situated in the GTP-binding pocket of U5-116kD, and Cys478 and Leu637 form internal contacts in domains II and III, respectively. Because individuals with alterations at these three positions demonstrate the full clinical presentation of MFDM, these three substitutions are presumed to cause a substantial derangement of U5-116kD function and/or stability.

U5-116kD alterations are uniquely pleiotropic in contrast to the range of previously reported spliceosomal phenotypes in humans. Interestingly, all four of the other spliceosomal subunits known to produce a clinical phenotype in humans (*PRPF31* [MIM 606419], *PRPF8* [MIM 607300], *SNRNP200* [MIM 601664], and *PRPF6* [MIM 613979]) cause retinitis pigmentosa, an isolated retinal condition.[18–21] The reason for this difference in phenotypes remains unexplained because *PRPF8* and, in particular, *SNRNP200* encode the human homologs of Prp8p and Brr2p—two RNA helicases that complex with (and are regulated by) U5-116kD.[11–14] Considering that splicing is an obligatory process for gene expression in all cells, the pertinent question is not why *EFTUD2* mutations cause a multiple-malformation syndrome with intellectual disability, but rather why the same is not seen for all other spliceosomal constituents. The developmental significance of splicing defects has been similarly illustrated for the minor spliceosome with the discovery of mutations in a noncoding RNA gene, *RNU4ATAC*, as the cause of a syndromic skeletal dysplasia, microcephalic osteodysplastic primordial dwarfism type I (MIM 210710).[22] Because the U5 snRNP is common to both major and minor spliceosomes,[23] U5-116kD and the retinopathy-associated products of *PRPF8* and *SNRNP200* are expected to participate in both U2- and U12-dependent splicing reactions.

In addition to extending the range of reported spliceosomal phenotypes, our results also highlight a pathway affecting craniofacial development. Supported by observations of the *Tcof1*$^{+/-}$ mouse, the prevailing view of mandibulofacial dysostosis holds MFD to be a consequence of inadequate ribosome biogenesis in a vulnerable population of neural-crest precursors.[24] In keeping with

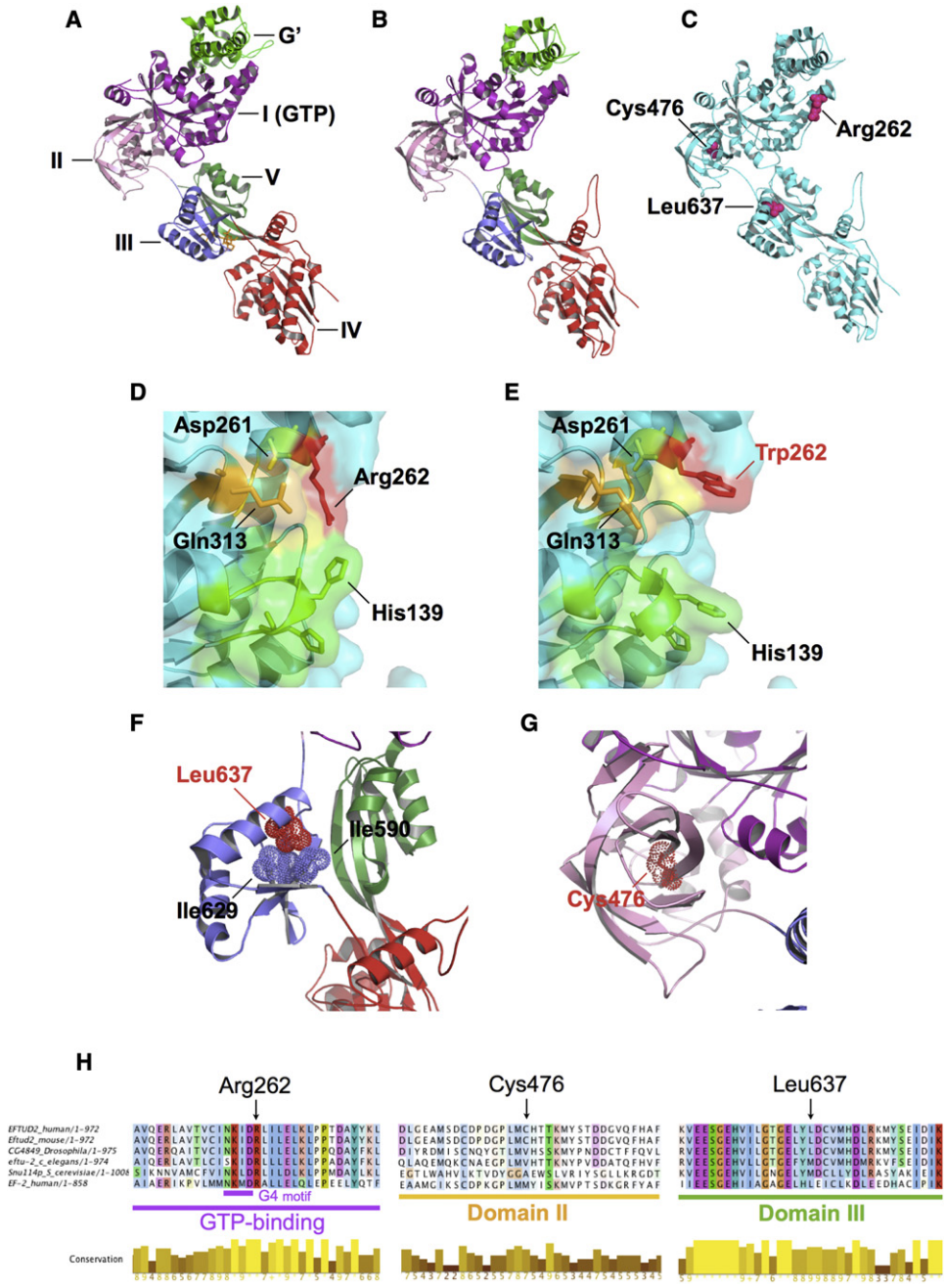

Figure 3. Predicted Structural Effects of MFDM-Causing Missense Mutations

We modeled residues 114–957 of EFTUD2 on the crystal structure of *S. cerevisiae* ribosomal elongation factor 2 (eEF2)[14] by using ModWeb, and we visualized them in PyMol.

(A) Crystal structure of eEF2 (PDB: 1N0U) complexed with the translation inhibitor sordarin (yellow). Structural domains are highlighted.

(B) U5-116kD model based on eEF2. The modeled portion of U5-116kD has high identity (37%) with eEF2; ModWeb scores this model as "reliable" (GA341 score is 1.00).

(C) Locations of amino acid substitutions p.Arg262Trp, p.Cys476Arg, and p.Leu637Arg.

(D) Arg262 (red) is predicted to occupy surface of GTP binding site. Also highlighted are additional surface-facing residues of G1 (green), G4 (yellow), and G5 (orange) motifs.

(E) Arg262Trp alteration in individual 2 is predicted to alter GTP-binding surface topology.

(F) Leu637 sidechain (helix II of domain III) is predicted to face inward and to form close hydrophobic contacts with Ile590 and Ile629. Leu637Arg (individual 11) is predicted to introduce a positive charge at this location.

(G) Cys476 is situated at the center of domain II's β barrel structure. p.Cys476Arg (individual 12) is predicted to introduce a positive charge at this position.

(H) Multispecies alignments of U5-116kDa illustrate sequence conservation in the vicinity of missense mutations identified in individuals with MFDM.

this, craniofacial malformations akin to those found in Treacher Collins syndrome are indeed seen in a subset of individuals with Diamond Blackfan anemia (MIM 105650), a ribosomopathy caused by alterations in any of several ribosomal subunits.[25] Whether altered ribosome biogenesis is an underlying aspect of the MFDM phenotype, and whether this is a direct or downstream effect remains to be determined; nonetheless, our findings point to an alternative pathway for investigating individuals with unexplained Treacher Collins syndrome and related conditions.

In summary, we have shown that de novo dominant mutations in *EFTUD* cause MFDM, a recognizable mandibulofacial dysostosis distinguished from Treacher Collins syndrome by microcephaly, global developmental delay, and a characteristic pattern of additional malformations. Because the participants in our study were selected on the basis of a highly specific presentation, the full clinical spectrum of MFDM is unknown. Given the apparent high sensitivity of molecular testing in this condition, we suggest that this syndrome should be entertained in the differential diagnosis of any child with progressive microcephaly accompanied by craniofacial malformations.

Supplemental Data

Supplemental Data include two figures and one table and can be found with this article online at http://www.cell.com/AJHG.

Acknowledgments

The authors would first like to thank the study participants and their families, without whose participation this work would not be possible. This work was funded by the government of Canada through Genome Canada, the Canadian Institutes of Health Research (CIHR), and the Ontario Genomics Institute (OGI-049). Additional funding was provided by Genome Quebec, Genome British Columbia, and the Physicians' Services Incorporated Foundation. This work was part of the CRANIRARE Network funded through a grant from the German Ministry of Research and Education to D.R.L. and D.W. (BMBF 01GM0802). K.M.B. is supported by a Clinical Investigatorship Award from the CIHR Institute of Genetics. This work was selected for study by the FORGE Canada Steering Committee, consisting of K. Boycott (University of Ottawa), J. Friedman (University of British Columbia), J. Michaud (University of Montréal), F. Bernier (University of Calgary), M. Brudno (University of Toronto), B. Fernandez (Memorial University), B. Knoppers (McGill University), M. Samuels (Université de Montréal), and S. Scherer (University of Toronto). We would like to thank Janet Marcadier (clinical coordinator) for her contribution to the infrastructure of the FORGE Canada Consortium. We also wish to acknowledge the contribution of the high-throughput sequencing platform of the McGill University and Génome Québec Innovation Centre, Montréal, Canada.

Received: October 27, 2011
Revised: December 12, 2011
Accepted: December 30, 2011
Published online: February 2, 2012

Web Resources

The URLs for data presented herein are as follows:

Berkeley Drosophila Genome Project, Splice Site Prediction by Neural Network, http://www.fruitfly.org/seq_tools/splice.html
Database of Genomic Variants, http://projects.tcag.ca/variation/
DECIPHER v5.1, http://decipher.sanger.ac.uk/
FASTX-Toolkit, http://hannonlab.cshl.edu/fastx_toolkit/
NHLBI Exome Variant Server, http://evs.gs.washington.edu/EVS/
ModWeb, http://modbase.compbio.ucsf.edu/ModWeb20-html/modweb.html
Online Mendelian Inheritance in Man (OMIM), http://www.omim.org/
Picard, http://picard.sourceforge.net/
PyMol, http://www.pymol.org/
SAMtools, http://samtools.sourceforge.net/
UCSC Genome Browser, http://genome.ucsc.edu/cgi-bin/hgGateway/

References

1. The Treacher Collins Syndrome Collaborative Group. (1996). Positional cloning of a gene involved in the pathogenesis of Treacher Collins syndrome. Nat. Genet. *12*, 130–136.
2. Dauwerse, J.G., Dixon, J., Seland, S., Ruivenkamp, C.A., van Haeringen, A., Hoefsloot, L.H., Peters, D.J., Boers, A.C., Daumer-Haas, C., Maiwald, R., et al. (2011). Mutations in genes encoding subunits of RNA polymerases I and III cause Treacher Collins syndrome. Nat. Genet. *43*, 20–22.
3. Ng, S.B., Buckingham, K.J., Lee, C., Bigham, A.W., Tabor, H.K., Dent, K.M., Huff, C.D., Shannon, P.T., Jabs, E.W., Nickerson, D.A., et al. (2010). Exome sequencing identifies the cause of a mendelian disorder. Nat. Genet. *42*, 30–35.
4. Guion-Almeida, M.L., Zechi-Ceide, R.M., Vendramini, S., and Tabith Júnior, A. (2006). A new syndrome with growth and mental retardation, mandibulofacial dysostosis, microcephaly, and cleft palate. Clin. Dysmorphol. *15*, 171–174.
5. Wieczorek, D., Gener, B., González, M.J., Seland, S., Fischer, S., Hehr, U., Kuechler, A., Hoefsloot, L.H., de Leeuw, N., Gillessen-Kaesbach, G., and Lohmann, D.R. (2009). Microcephaly, microtia, preauricular tags, choanal atresia and developmental delay in three unrelated patients: a mandibulofacial dysostosis distinct from Treacher Collins syndrome. Am. J. Med. Genet. A. *149A*, 837–843.
6. Guion-Almeida, M.L., Vendramini-Pittoli, S., Passos-Bueno, M.R., and Zechi-Ceide, R.M. (2009). Mandibulofacial syndrome with growth and mental retardation, microcephaly, ear anomalies with skin tags, and cleft palate in a mother and her son: autosomal dominant or X-linked syndrome? Am. J. Med. Genet. A. *149A*, 2762–2764.
7. Li, H., and Durbin, R. (2009). Fast and accurate short read alignment with Burrows-Wheeler transform. Bioinformatics *25*, 1754–1760.
8. Li, H., Handsaker, B., Wysoker, A., Fennell, T., Ruan, J., Homer, N., Marth, G., Abecasis, G., and Durbin, R.; 1000 Genome Project Data Processing Subgroup. (2009). The Sequence Alignment/Map format and SAMtools. Bioinformatics *25*, 2078–2079.
9. Wang, K., Li, M., and Hakonarson, H. (2010). ANNOVAR: Functional annotation of genetic variants from high-throughput sequencing data. Nucleic Acids Res. *38*, e164.

10. Fabrizio, P., Laggerbauer, B., Lauber, J., Lane, W.S., and Lührmann, R. (1997). An evolutionarily conserved U5 snRNP-specific protein is a GTP-binding factor closely related to the ribosomal translocase EF-2. EMBO J. *16*, 4092–4106.
11. Häcker, I., Sander, B., Golas, M.M., Wolf, E., Karagöz, E., Kastner, B., Stark, H., Fabrizio, P., and Lührmann, R. (2008). Localization of Prp8, Brr2, Snu114 and U4/U6 proteins in the yeast tri-snRNP by electron microscopy. Nat. Struct. Mol. Biol. *15*, 1206–1212.
12. Achsel, T., Ahrens, K., Brahms, H., Teigelkamp, S., and Lührmann, R. (1998). The human U5-220kD protein (hPrp8) forms a stable RNA-free complex with several U5-specific proteins, including an RNA unwindase, a homologue of ribosomal elongation factor EF-2, and a novel WD-40 protein. Mol. Cell. Biol. *18*, 6756–6766.
13. Bartels, C., Klatt, C., Lührmann, R., and Fabrizio, P. (2002). The ribosomal translocase homologue Snu114p is involved in unwinding U4/U6 RNA during activation of the spliceosome. EMBO Rep. *3*, 875–880.
14. Small, E.C., Leggett, S.R., Winans, A.A., and Staley, J.P. (2006). The EF-G-like GTPase Snu114p regulates spliceosome dynamics mediated by Brr2p, a DExD/H box ATPase. Mol. Cell *23*, 389–399.
15. Bartels, C., Urlaub, H., Luhrmann, R., and Fabrizio, P. (2003). Mutagenesis suggests several roles of Snu114p in pre-mRNA splicing. J. Biol. Chem. *278*, 28324–28334.
16. Brenner, T.J., and Guthrie, C. (2005). Genetic analysis reveals a role for the C terminus of the *Saccharomyces cerevisiae* GTPase Snu114 during spliceosome activation. Genetics *170*, 1063–1080.
17. Jørgensen, R., Ortiz, P.A., Carr-Schmid, A., Nissen, P., Kinzy, T.G., and Andersen, G.R. (2003). Two crystal structures demonstrate large conformational changes in the eukaryotic ribosomal translocase. Nat. Struct. Biol. *10*, 379–385.
18. Vithana, E.N., Abu-Safieh, L., Allen, M.J., Carey, A., Papaioannou, M., Chakarova, C., Al-Maghtheh, M., Ebenezer, N.D., Willis, C., Moore, A.T., et al. (2001). A human homolog of yeast pre-mRNA splicing gene, *PRP31*, underlies autosomal dominant retinitis pigmentosa on chromosome 19q13.4 (RP11). Mol. Cell *8*, 375–381.
19. McKie, A.B., McHale, J.C., Keen, T.J., Tarttelin, E.E., Goliath, R., van Lith-Verhoeven, J.J., Greenberg, J., Ramesar, R.S., Hoyng, C.B., Cremers, F.P., et al. (2001). Mutations in the pre-mRNA splicing factor gene *PRPC8* in autosomal dominant retinitis pigmentosa (RP13). Hum. Mol. Genet. *10*, 1555–1562.
20. Zhao, C., Bellur, D.L., Lu, S., Zhao, F., Grassi, M.A., Bowne, S.J., Sullivan, L.S., Daiger, S.P., Chen, L.J., Pang, C.P., et al. (2009). Autosomal-dominant retinitis pigmentosa caused by a mutation in *SNRNP200*, a gene required for unwinding of U4/U6 snRNAs. Am. J. Hum. Genet. *85*, 617–627.
21. Tanackovic, G., Ransijn, A., Ayuso, C., Harper, S., Berson, E.L., and Rivolta, C. (2011). A missense mutation in *PRPF6* causes impairment of pre-mRNA splicing and autosomal-dominant retinitis pigmentosa. Am. J. Hum. Genet. *88*, 643–649.
22. He, H., Liyanarachchi, S., Akagi, K., Nagy, R., Li, J., Dietrich, R.C., Li, W., Sebastian, N., Wen, B., Xin, B., et al. (2011). Mutations in U4atac snRNA, a component of the minor spliceosome, in the developmental disorder MOPD I. Science *332*, 238–240.
23. Schneider, C., Will, C.L., Makarova, O.V., Makarov, E.M., and Lührmann, R. (2002). Human U4/U6.U5 and U4atac/U6atac.U5 tri-snRNPs exhibit similar protein compositions. Mol. Cell. Biol. *22*, 3219–3229.
24. Dixon, J., Jones, N.C., Sandell, L.L., Jayasinghe, S.M., Crane, J., Rey, J.P., Dixon, M.J., and Trainor, P.A. (2006). Tcof1/Treacle is required for neural crest cell formation and proliferation deficiencies that cause craniofacial abnormalities. Proc. Natl. Acad. Sci. USA *103*, 13403–13408.
25. Gazda, H.T., Sheen, M.R., Vlachos, A., Choesmel, V., O'Donohue, M.F., Schneider, H., Darras, N., Hasman, C., Sieff, C.A., Newburger, P.E., et al. (2008). Ribosomal protein L5 and L11 mutations are associated with cleft palate and abnormal thumbs in Diamond-Blackfan anemia patients. Am. J. Hum. Genet. *83*, 769–780.